

E1 transitions in ^{17}F . I. The low-lying $T = \frac{3}{2}$ states*

M. N. Harakeh, P. Paul, and K. A. Snover†

Department of Physics, State University of New York, Stony Brook, New York 11794

(Received 5 November 1974)

The $^{16}\text{O}(p, \gamma_0, i)^{17}\text{F}$ reaction was studied in the region of previously reported low-lying $T = \frac{3}{2}$ states in ^{17}F . Resonances were observed at $E_p = 11.275 \pm 0.006$, 12.711 ± 0.006 , 13.255 ± 0.006 , 14.435 ± 0.010 , and 14.583 ± 0.006 MeV with $(2J_R + 1)\Gamma_{P_0}\Gamma_\gamma/\Gamma = 1.2 \pm 0.4$, 13.6 ± 3.5 , 2.5 ± 1.5 , 13.0 ± 5.9 , and 11.8 ± 5.3 eV, respectively. Using reported values for $(2J_R + 1)\Gamma_{P_0}/\Gamma$, radiative widths $\Gamma_\gamma = 6.0 \pm 2.5$, 11.3 ± 3.4 , 2.8 ± 1.8 , 81 ± 54 , and 13.4 ± 7.0 eV were deduced for the respective resonances. Shell model 2p-1h calculations using realistic Kuo-Brown interaction matrix elements were performed. The computed excitation energies and $B(E1)$ values were found to agree with the experimental results.

NUCLEAR STRUCTURE ^{17}F ; measured $^{16}\text{O}(p, \gamma)$; deduced E_x , Γ , $(2J_R + 1)\Gamma_p \Gamma_\gamma/\Gamma$ of $^{17}\text{F}(T = \frac{3}{2})$ levels. 2p-1h calculations performed for negative parity $^{17}\text{F}(T = \frac{3}{2})$ levels; compared theoretical $B(E1)$ matrix elements to experimentally deduced values.

I. INTRODUCTION

It is well known that electric dipole ($E1$) transitions between low-lying single-particle (s.p.) states are systematically hindered compared to the s.p. estimates. This can be phenomenologically expressed by an effective $E1$ charge in analogy to the well-established $E2$ effective charges.¹ These effective charges are believed to arise from the coupling of the s.p. excitation to collective core excitations. While in the case of low-lying $E2$ transitions the isoscalar collective $E2$ state enhances the s.p. transition, the isovector collective $E1$ excitations are thought to deplete the strength of the low-lying $E1$ transitions. This model can be accurately tested in the case of $E1$ transitions because the collective core effects are mainly due to the giant dipole resonance (GDR) which is well understood both experimentally and theoretically. In simple nuclei (those neighboring closed-shell nuclei) collective effects can be included explicitly. For instance, in case of one extra nucleon 2p-1h excitations have to be included in addition to the 1p excitations. This has been done in nuclei near $A = 90$ with quantitative success for the collective dipole states as well as the $E1$ transitions from low-lying states.² However, because of the many excitations that often have to be included in heavy nuclei the collective effects have mostly been treated in a phenomenological model, with good systematic success.

In light nuclei a comprehensive microscopic theoretical treatment is in principle quite feasible

but has not previously been attempted partially because few data on isospin-allowed $E1$ transitions from low-lying states were available and also because the localization of collective dipole strength in the $T = \frac{1}{2}$ and $T = \frac{3}{2}$ isospin components was not well understood.

The nucleus ^{17}F is a good case for such a study. Recently detailed studies of the first few $T = \frac{3}{2}$ states in ^{17}F were published.^{3,4} Figure 1 shows the level diagram of the reported states with their assigned spins and parities. Obviously most of these states can decay by an $E1$ transition to the ground and/or first excited state. Since the pertinent particle parameters are known for those states from elastic proton scattering, radiative widths may be obtained from a study of the radiative capture reaction $^{16}\text{O}(p, \gamma)^{17}\text{F}$. These measurements are discussed in Secs. II and III.

Even in the lowest order these states have 2p-1h character and are thus not strictly s.p. states. Nevertheless, the coupling to the collective mode should be present and have the same effect as discussed for s.p. states at the beginning. The appropriate collective excitation should be the $T = \frac{3}{2}$ component of the GDR. To explore this quantitatively, theoretical predictions for the $E1$ widths are derived in Sec. IV of this paper in a 2p-1h microscopic model using various Kuo-Brown realistic interactions in a basis of good isospin. It will be shown that the widths so calculated are in agreement with the data for the low-lying $T = \frac{3}{2}$ transitions. At the same time, these calculations include predictions for the collective $T = \frac{1}{2}$ and $T = \frac{3}{2}$

dipole states, and these will be compared with results from radiative capture studies at higher energies in a second paper (see following paper).

II. EXPERIMENTAL PROCEDURE

Because the widths of the resonances under study ranged from 1 to 40 keV, thin self-supporting oxygen targets were needed. These were obtained by complete oxidation of thin Ni foils in an oxygen atmosphere using a focused light beam. After oxidation the foils became semitransparent with a uniform bluish-green color. Different thicknesses were produced by starting with different Ni foils. The thickness of the thickest target used was measured before and after oxidation by determining the equivalent amount of air needed to stop 5.5-MeV α particles from an ^{241}Am source. This effective thickness changed from $722 \pm 16 \mu\text{g}/\text{cm}^2$ before to $919 \pm 16 \mu\text{g}/\text{cm}^2$ after oxidation. The $197 \pm 22 \mu\text{g}/\text{cm}^2$ of oxygen added to the target are in correct proportion to the original number of Ni atoms required for the complete formation of NiO. The thickness of thinner targets was then obtained by comparing the yields from the $\text{Ni}(p, \gamma)$ and $^{16}\text{O}(p, p')^{16}\text{O}^*(6.13 \text{ MeV})$ reactions to the same yields from the "thick" target. In this way, a

"medium" thick target gave $228 \pm 5 \mu\text{g}/\text{cm}^2$ of Ni and $62 \pm 7 \mu\text{g}/\text{cm}^2$ of O, and a "thin" target $120 \pm 3 \mu\text{g}/\text{cm}^2$ of Ni to $32.6 \pm 3.6 \mu\text{g}/\text{cm}^2$ of O. All of the ratios are consistent with full oxidation.

In order to evaluate background effects SiO foils were also used but all absolute cross section determinations were made with NiO targets.

The proton beam of the Stony Brook tandem was used to cover a bombarding energy range from 11.0 to 14.8 MeV. The energy resolution of the beam was obtained by tracing out the very narrow⁵ (0.9 keV) resonance⁶ at $E_p = 14.231 \text{ MeV}$ in the $^{12}\text{C}(p, \gamma)^{13}\text{N}$ reaction, and was measured to be about 2.7 keV. Beam currents were limited by the detector counting rates to between 50 and 200 nA.

γ rays of energy between 11 and 14 MeV were detected in a 25-cm \times 25-cm NaI crystal with anticoincidence shield⁷ and the electronically accepted and rejected γ spectra were recorded in two halves of a multichannel analyzer. The detector resolution for a 15.1-MeV γ ray was $\sim 5\%$, worse than the values of which the detector was capable but adequate for the experiment. The ratio of accepted to total pulses in the region of interest was ~ 0.65 .

The main detection problem comes from the low Q value of the $^{16}\text{O}(p, \gamma)^{17}\text{F}$ reaction (0.60 MeV) which means that almost any suitable target back-

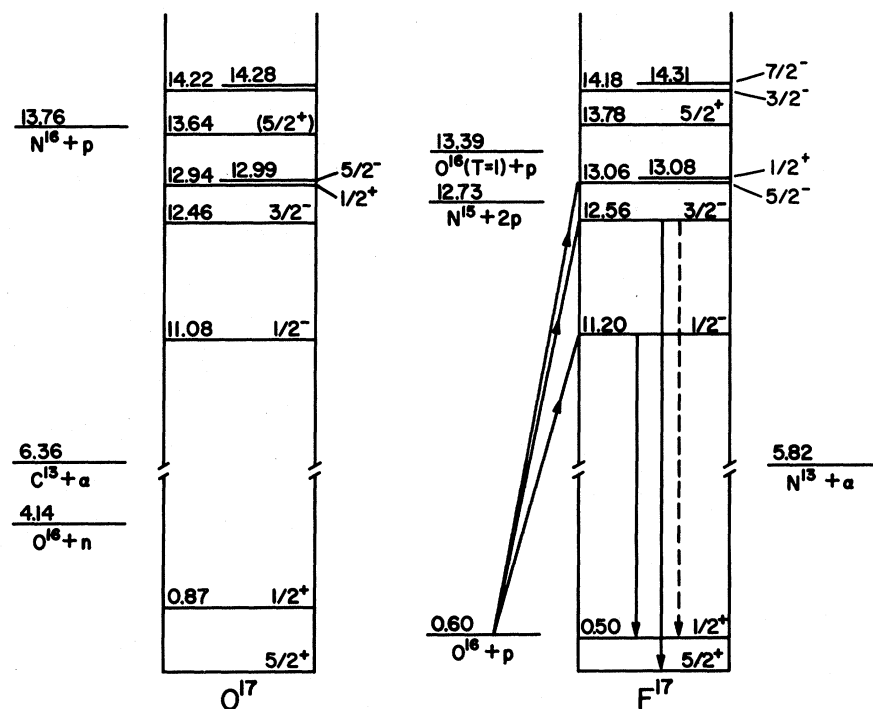


FIG. 1. $T = \frac{3}{2}$ levels and Q values (all in MeV) in ^{17}F and ^{17}O which are pertinent to the present radiative proton capture study.

ing material will produce γ rays of higher energy. However, a run on unoxidized Ni showed the γ spectrum to be quite flat where the ^{17}F γ rays would be expected. Figure 2 shows two spectra, taken on top of the $E_p = 12.711$ MeV resonance and 21 keV below. The high energy parts of both spectra indicate the radiative capture peaks on the various Ni isotopes from the backing. On resonance, the unresolved transitions to the ground state and/or first excited state at 500 keV in ^{17}F are clearly seen. Although separation of both transitions was beyond the capability of the Stony Brook γ spectrometer at its best, a careful energy calibration enabled us to establish which transition was dominant at each of the resonances. The transition strength was, however, always extracted from the entire observed peak, thus summing both transitions.

The capture cross sections were obtained from an absolute calibration of the detector and checked against the $^{12}\text{C}(p, \gamma)^{13}\text{N}$ reaction at the 14.231-MeV resonance whose integrated cross section is given by⁶ $\Gamma_{p_0} \Gamma_\gamma / \Gamma = 5.5 \pm 0.8$ eV. We find that the extrapolation of line shapes from 15.1 MeV to the lower γ -ray energies, extrapolation of line shapes tails, beam current integration, and the uncertainty in attenuation of γ rays between target and NaI crystal

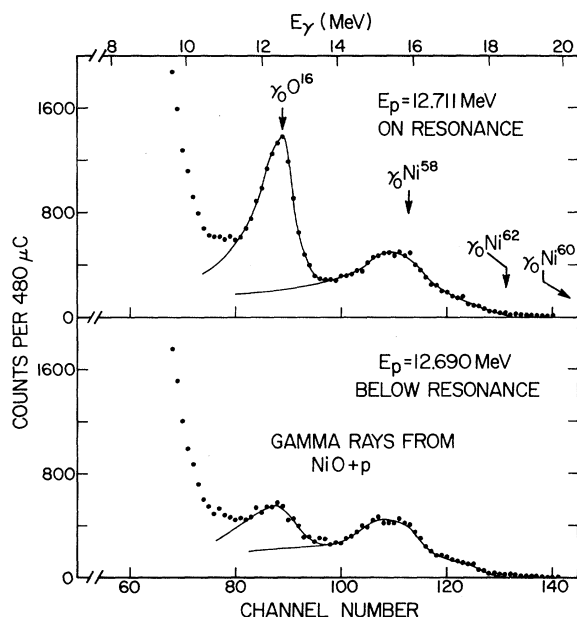


FIG. 2. γ -ray spectra obtained in the proton bombardment of a thin NiO target at the 12.711-MeV resonance (top) and just below (bottom). The resonant γ transition from $^{16}\text{O}(p, \gamma)^{17}\text{F}$ and the energies of various expected background peaks from the Ni isotopes are indicated. The results of a fitting procedure using a standard line shape for the ^{17}F transition and a smooth background are drawn into the spectra.

TABLE I. Location and width of $T = \frac{3}{2}$ resonances in ^{17}F observed in $^{16}\text{O}(p, \gamma)^{17}\text{F}$ and (in parentheses) $^{16}\text{O}(p, p)$. The spin and parity assignments are from elastic scattering (Refs. 3 and 4).

E_p (MeV)	E_x (MeV)	Γ (keV)	J^π
11.275 ± 0.006 (11.267 ± 0.007) ^a	11.204 ± 0.006	≤ 1.6 (0.5)	$\frac{1}{2}^-$
12.711 ± 0.006 (12.713 ± 0.007) ^a (12.708 ± 0.004) ^b	12.554 ± 0.006	1.8 ± 0.5 (1.8) ^a (3 ± 1) ^b	$\frac{3}{2}^-$
13.255 ± 0.006 (13.250 ± 0.004) ^b	13.065 ± 0.006	5.0 ± 1.5 (2 ± 1)	$\frac{5}{2}^-$
Not observed (13.271 ± 0.004) ^b		(2 ± 1)	($\frac{1}{2}^+$)
Not observed (14.017 ± 0.004) ^b		(12 ± 5)	$\frac{5}{2}^+$
14.435 ± 0.010 (14.438 ± 0.006) ^b	14.174 ± 0.010	41 ± 10 (27 ± 5)	$\frac{3}{2}^-$ ($\frac{1}{2}^-$)
14.583 ± 0.006 (14.579 ± 0.010) ^b	14.313 ± 0.006	28 ± 5 (20 ± 5)	$\frac{7}{2}^-$

^a From Ref. 4.

^b From Ref. 3.

introduce a maximal systematic error of $\pm 15\%$. The errors arising from target thickness, total width determination, statistics, and angular distributions will be considered separately for each resonance.

III. EXPERIMENTAL RESULTS

Table I lists the energies and widths of proton capture resonances in ^{17}F which have been observed in the present work from thin and thick target excitation functions. For comparison, the $T = \frac{3}{2}$ resonances in ^{17}F obtained from elastic proton scattering^{3, 4} over the same range of bombarding energies are listed with the given widths and J^π assignments. With the exception of the resonances reported at 13.271 and 14.017 MeV which were not observed in the proton capture reaction, there is general agreement in the widths and resonance energies between the present work and the elastic scattering results. Table I lists also the excitation energies in ^{17}F which were derived from the resonance energies by use of the relativistically corrected (to first order) formula:

$$E_x = Q + D - \frac{D^2}{2(m_1 + m_2)}, \quad (1)$$

where $D = [m_1 / (m_1 + m_2)] E_p$, and Q is the reaction Q value, m_1 and m_2 are target and projectile masses, respectively, and E_p is the lab energy of the

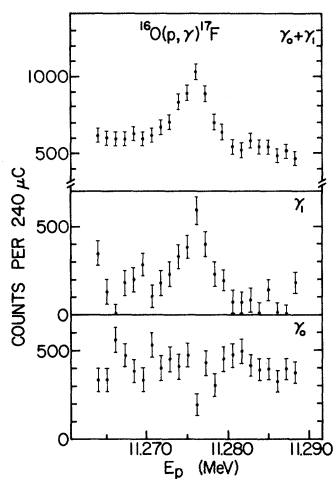


FIG. 3. Excitation function of the $^{16}\text{O}(p, \gamma)^{17}\text{F}$ reaction over the very narrow (500 eV) 11.275-MeV resonance. A line shape analysis shows that the sum peak of $\gamma_0 + \gamma_1$ (top) really resonates only in the γ_1 transition (center).

projectile. For a comparison of these excitation energies with those of other members of the $A=17$ isobaric multiplet, we refer to the detailed discussion in Ref. 3. We note that all resonances which are observed in radiative capture have previously assigned^{3,4} negative parity and spin assignments which permit decay by an $E1$ transition to the ground state ($\frac{5}{2}^+$) or the first excited state ($\frac{1}{2}^+$), and that those known resonances not observed in radiative capture would involve $M1$ or $E2$ decay. The data obtained for each resonance will now briefly be discussed case by case, with a general discussion of the extraction of resonance strengths following at the end of this section.

11.275 MeV. The (p, γ) excitation curve over this resonance obtained with the thinnest target is shown in Fig. 3. As detailed analysis of the γ spectra shows, the resonance decays only to the first excited state, consistent with $E1$ γ emission and the $J^\pi = \frac{1}{2}^-$ assignment reported^{4,8} for the resonance.

12.711 MeV. This is the strongest of all observed resonances and results are shown in Fig. 4 for a thick and a thin target. Runs were also taken here with a large Ge(Li) detector to help establish the branching ratio of the ground and first excited states; however, the 500-keV energy difference between γ_0 and γ_1 and the consequent overlap of peaks in the Ge(Li) spectrum limited the accuracy of this measurement. The result for the relative resonant yield is $Y(\gamma_1)/Y(\gamma_0 + \gamma_1) = 0.20 \pm 0.05$.

Measured angular distributions on and just below resonance are shown in Fig. 5. Good fits were obtained with a Legendre polynomial expansion using

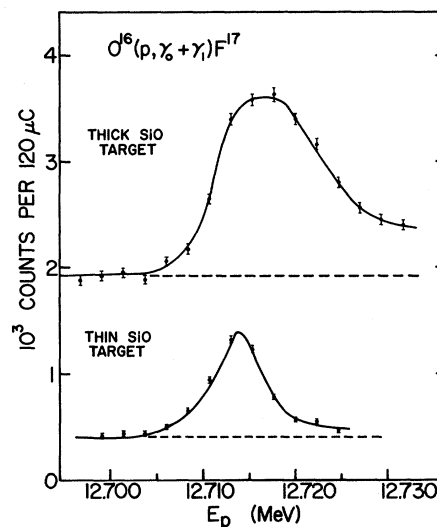


FIG. 4. Summed $\gamma_0 + \gamma_1$ yield function over the 1.8-keV wide resonance at 12.711 MeV.

even terms up to order 2 and gave the values $W(\theta, \text{on res.}) = 1 - (0.67 \pm 0.09)P_2(\cos \theta)$, $W(\theta, \text{below res.}) = 1 - (0.56 \pm 0.36)P_2(\cos \theta)$. A subtraction of these angular distributions normalized to the yields on and below resonance gives the angular distribution of the resonant contribution $W(\theta, \text{res.}) = 1 - (0.70 \pm 0.23)P_2$. Assuming an isolated resonance with the reported^{3,4} assignments $J^\pi = \frac{3}{2}^-$ the predicted a_2 coefficient is $a_2 = -0.1$ for the γ_0 transition and $a_2 = -0.5$ for the γ_1 transition, which is clearly incompatible with the measured angular distributions and the γ_1/γ_0 branching ratio given above. Since the spin assignment appears to be

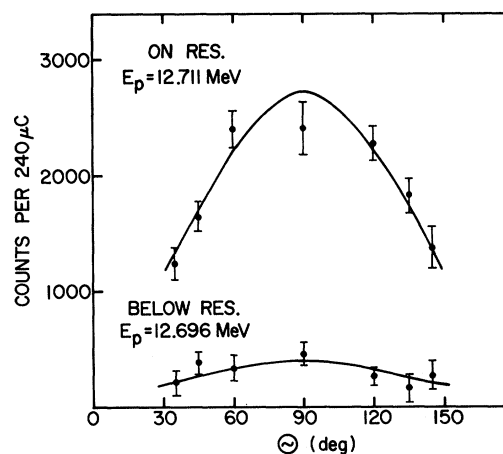


FIG. 5. Angular distributions of the $\gamma_0 + \gamma_1$ yield at and just below the 12.711-MeV resonance. Solid curves are fits corresponding to $W(\theta) = 1 - (0.67 \pm 0.09)P_2(\cos \theta)$ on resonance, and $W(\theta) = 1 - (0.56 \pm 0.36)P_2(\cos \theta)$ below resonance.

quite reliable, the most likely explanation lies in interference with the background. For example, if the background is produced by capture of an $f_{7/2}$ wave, then both the on and off resonance angular distributions can be reproduced with a relative phase factor of $\cos\phi = 0.78$ between the resonance and the background amplitudes. The resulting resonant amplitude A_R would then be reduced by 24% below the value inferred from the 90° data without interference. If, on the other hand, the resonant amplitude is extracted from the total cross section, i.e., using the measured angular distribution $W(\theta, \text{res.})$, neglecting interference, one obtains a value within 5% of A_R . Arbitrarily then, an error of $\pm 10\%$ was included for the strength of this resonance to cover this uncertainty.

At the other resonances the yields were too low to measure angular distributions with meaningful accuracy. Thus the theoretical angular distributions were used for these cases in the extraction of radiative widths, from the 90° data, and an uncertainty of $\pm 25\%$ was used to account for possible interference effects.

13.250 and 13.271 MeV. Data taken over these two reported resonances are shown in Fig. 6. The

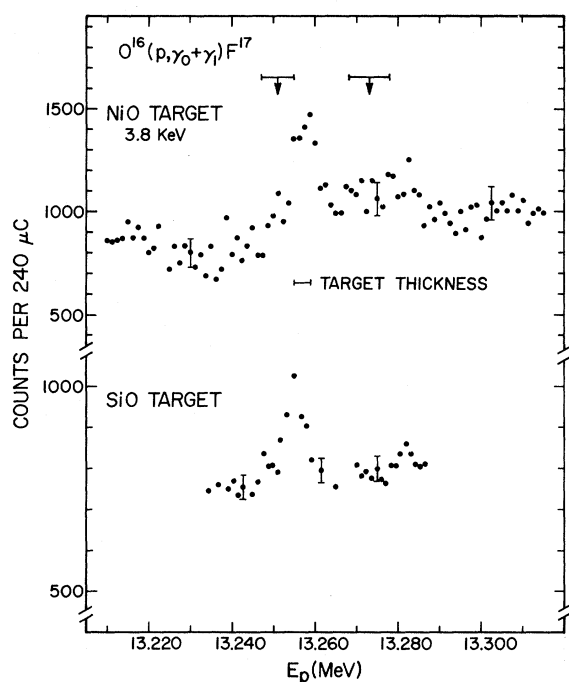


FIG. 6. Excitation function for the summed transitions over the region of the reported resonances at $E_p = 13.250$ ($J = \frac{5}{2}^-$) and 13.271 ($J = \frac{1}{2}^+$) indicated by arrows with the published uncertainties. A single resonance, observed at 13.255 MeV, is associated with the negative-parity state. The positive-parity resonance which could decay by an $M1$ or $E2$ transition is not observed.

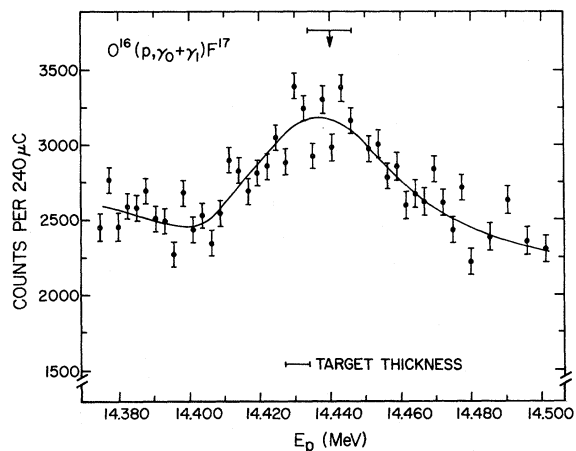


FIG. 7. Summed $\gamma_0 + \gamma_1$ yield curve over the resonance reported at 14.438 MeV (see arrow). The present observed width of 41 keV is somewhat larger than the reported value (27 keV).

arrows indicate the locations reported in Ref. 3. The location observed in capture is clearly higher by 5 keV, in agreement with the position reported by Van Bree.⁴ The resonance decay connects predominantly ($> 50\%$) to the ground state, compatible with the $J^\pi = \frac{5}{2}^-$ assignment.

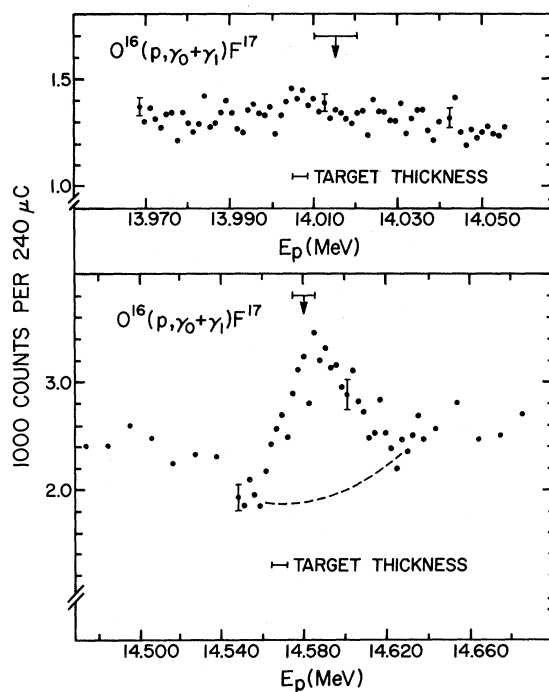


FIG. 8. γ yield over the region of the reported resonances at $E_p = 14.017$ MeV (top) and 14.579 MeV (bottom) indicated by arrows. While the first resonance (positive parity) is not seen in the γ yield, the second one (negative parity) is strong.

TABLE II. Resonance strengths and radiative widths of $T = \frac{3}{2}$ resonances observed in the $^{16}\text{O}(p, \gamma_0 + \gamma_1)^{17}\text{F}$ reaction. J^π assignments and Γ_{p_0}/Γ ratios which enter into the extraction of Γ_γ are generally taken from Ref. 3. The branching ratios for γ_0 and γ_1 are discussed in the text.

E_p (MeV)	J^π	$(2J_r + 1) \frac{\Gamma_{p_0} \Gamma_\gamma}{\Gamma}$ (eV)	Γ_{p_0}/Γ	Γ_γ (eV)
11.275	$\frac{1}{2}^-$	1.2 ± 0.4	0.1 ± 0.02^a	6.0 ± 2.5
12.711	$\frac{3}{2}^-$	13.6 ± 3.5	0.30 ± 0.05^a (0.26 ± 0.04)	11.3 ± 3.4
13.255	$\frac{5}{2}^-$	2.5 ± 1.5	0.15 ± 0.4	2.8 ± 1.8
13.271	$(\frac{1}{2}^+)$	≤ 0.56	0.04 ± 0.02	≤ 7
14.017	$\frac{5}{2}^+$	≤ 1.42	0.02 ± 0.01	≤ 11.8
14.435	$(\frac{1}{2}^-), \frac{3}{2}^-$	13.0 ± 5.9	0.04 ± 0.02	81 ± 54
14.583	$\frac{7}{2}^-$	11.8 ± 5.3	0.11 ± 0.03	13.4 ± 7.0

^a From Ref. 4.

The second reported resonance is not observed in radiative capture. It has a very small reported value for $\Gamma_{p_0}/\Gamma = 0.04$, and could only decay by $M1/E2$ radiation.

14.435 MeV. This resonance which is rather wide (42 keV) is shown in Fig. 7. A smooth background was subtracted to obtain the resonance strength. The dominant part of the decay strength at this energy goes to the ground state. However, because of the very large background under the resonance, it was impossible to ascertain whether the resonance itself decays to the ground state, which would have differentiated between the $\frac{1}{2}^-$ and $\frac{3}{2}^-$ assignments which are presently compatible with elastic proton scattering.³ This resonance has a value of $\Gamma_{p_0}/\Gamma = 0.04$ which is as small as that of the unobserved 13.271-MeV resonance and yet is observed strongly.

14.017 and 14.583 MeV. Arrows in Fig. 8 indicate the reported locations of these two resonances.³ The lower one which has $\Gamma_{p_0}/\Gamma = 0.02$ and could decay by an $M1/E2$ transition is again not observed in radiative capture. The higher one is very prominent and decays predominantly by γ_0 emission. The background shown in the figure was subtracted to obtain the resonance yield.

From the 90° yields the resonance capture strengths were computed using the relations⁹

$$(2J_R + 1) \frac{\Gamma_p \Gamma_\gamma}{\Gamma} = \frac{m_1}{m_1 + m_2} \frac{\epsilon}{\pi^2 \chi^2} Y(\infty), \quad (2)$$

$$Y(\infty) = Y(90^\circ) \frac{\pi}{2tg^{-1}(\xi/\Gamma)} \frac{1}{1 - a_2/2}, \quad (3)$$

where ϵ is the stopping power, m_1 and m_2 are target and projectile masses, ξ is the target thickness, and Γ is the total resonance width; a_2 is the computed or measured coefficient in the angular distribution. The observed yield at 90° $Y(90^\circ)$ can be obtained from the number of counts N in the appropriate figures by using $Y(90^\circ) = 3.5 \times 10^{-11} (N/Q)(\mu\text{C})$, where the numerical factor contains the total detector efficiency. The resulting capture strengths are given in Table II. Using reported values^{3,4} for Γ_{p_0}/Γ (and for consistency Γ values from the same references from which Γ_{p_0}/Γ were taken) and accepting the published spin assignments radiative widths Γ_γ are finally extracted and are listed in the last column. The over-all errors on these values are of the order of 50%. Table III presents a breakdown of the various error contributions which were added quadratically to yield the total error quoted in Table II for Γ_γ .

IV. CALCULATION OF E1 TRANSITION STRENGTHS IN ^{17}F

In ^{17}F , odd-parity states with $T = \frac{3}{2}$ can, of course, only be constructed by involving excitations of the ^{16}O core, thus involving in lowest or-

TABLE III. Percentage errors entering into the total percent error on Γ_γ for observed capture resonances in $^{16}\text{O}(p, \gamma)^{17}\text{F}$. The various quantities are defined in Eqs. (2) and (3) in the text. Errors on Γ_{p_0}/Γ are taken from Refs. 3 and 4. The final percentage error is obtained from $\sigma^2 = \sum_i \sigma_i^2$.

E_p (MeV)	Systematic	ϵ	$\int W(\theta) d\theta$	$Y(90^\circ)$	ξ	Γ	$\tan^{-1}(\xi/\Gamma)$	$(2J_R + 1) \frac{\Gamma_{p_0} \Gamma_\gamma}{\Gamma}$	Γ_{p_0}/Γ	Γ_γ
11.275	15	10	25	13.3	10	20 ^a	15.2	37	20 ^a	42
12.711	15	10	10	7.5	10	15 ^a	14.4	26	15 ^a	30
13.255	15	10	25	25	10	50 ^b	41.7	58	26.7 ^b	63
14.435	15	10	25	25	10	18.5 ^b	21	45	50 ^b	67
14.583	15	10	25	18.6	10	25 ^b	26.6	45	27 ^b	52

^a From Ref. 4.

^b From Ref. 3.

TABLE IV. Single-particle energies (in MeV) relative to the ^{16}O ground state which were used in the 2p-1h states calculation.

$1p_{3/2}$	$1p_{1/2}$	$1d_{5/2}$	$2s_{1/2}$	$1d_{3/2}$
-21.74	-15.60	-4.15	-3.28	0.93

der 2p-1h states. In fact, $A=17$ has been a favored test case for many particle-many hole (p-h) calculations. As far back as 1954¹⁰ and more recently^{11,12} the predominant 4p-3h nature of the lowest $\frac{1}{2}^-$ level was established. Several calculations have been performed since then on the low-lying ($T=\frac{1}{2}$) states, but only two^{13,14} included the lowest $T=\frac{3}{2}$ states and are therefore of interest here.

Margolis and deTakacsy¹³ computed all 2p-1h odd-parity states with the full ($1p$) and ($2s, 1d$) shells active. They used a Gillet type interaction and allowed for separate adjustment of the p-p and the p-h interaction. Soga¹⁴ used an effective interaction but considered only the $p_{1/2}$ shell active for holes and the $1d_{5/2}, 2s_{1/2}$ shell for particles, and only in restricted combinations so that $\frac{7}{2}^-$ states were not included. Exclusion of the $p_{3/2}$ shell is clearly too severe a restriction if one wishes to calculate γ transition strengths and in fact prevents the buildup of a coherent state, i.e., the GDR.

We have computed the spectrum of negative-parity $T=\frac{3}{2}$ states in ^{17}F up to $J=\frac{7}{2}$ in a 2p-1h basis with the entire ($1p$) and ($2s, 1d$) shells active and using a consistent set of realistic Kuo-Brown ma-

using the relation

$$\langle j_a^{-1}j_b, TJ | V^{\text{ph}} | j_c^{-1}j_d, TJ \rangle = (-1)^{j+1} \sum_{T_0 J_0} \hat{T}_0 \hat{J}_0 W(\frac{1}{2} \frac{1}{2} \frac{1}{2} \frac{1}{2}, TT_0) W(j_a j_b j_d j_c, JJ_0) \langle j_a j_d T_0 J_0 | V^{\text{pp}} | j_c j_b T_0 J_0 \rangle, \quad (6)$$

where $j=j_a+j_b+j_c+j_d$, $\hat{T}_0=2T_0+1$, and $\hat{J}_0=2J_0+1$.

Two sets of matrix elements were considered; one obtained from a soft-core Reid potential, the other from the Hamada-Johnston potential. Both gave very similar results which will be labeled as case I in the following discussion.

In a second approach (case II), p-h matrix elements identical to case I, but the renormalized particle-particle matrix elements¹⁵ in the (sd) shell were chosen so as to correctly fit the low-lying spectrum of ^{18}O and ^{18}F .

Coulomb effects were neglected in the calculation; their effect would be to move the entire spectrum down by 200–300 keV. To minimize this effect the spectrum was calculated for ^{17}O . We note that the problem of spurious states does not arise for the $T=\frac{3}{2}$ states (i.e., states of maximum isospin).

trix elements¹⁵ for the particle-particle and the particle-hole interaction. In this basis the Hamiltonian for the problem can be written as:

$$H = \sum_{\alpha} \epsilon_{\alpha} (a_{\alpha}^{\dagger} a_{\alpha} + b_{\alpha}^{\dagger} b_{\alpha}) + \sum_{\alpha\beta\gamma\delta} V_{\alpha\beta\gamma\delta}^{\text{pp}} a_{\alpha}^{\dagger} a_{\beta}^{\dagger} a_{\delta} a_{\gamma} + \sum_{\alpha\beta\gamma\delta} V_{\alpha\beta\gamma\delta}^{\text{ph}} a_{\alpha}^{\dagger} b_{\beta}^{\dagger} b_{\delta} a_{\gamma}, \quad (4)$$

where $a_{\alpha}^{\dagger} (b_{\alpha}^{\dagger})$ and $a_{\alpha} (b_{\alpha})$ are the usual creation and annihilation operators for particles (holes), ϵ_{α} is the single-particle (hole) energy, V^{pp} and V^{ph} are the particle-particle and particle-hole interaction, respectively.

The basis states are constructed in the following way in j - j coupling:

$$|j_{\alpha}^{-1}, j_{\beta} j_{\gamma} (J_1 T_1) T J \rangle = [b_{\alpha}^{\dagger} [a_{\beta}^{\dagger} a_{\gamma}^{\dagger}]_{J_1 T_1}]_{JT}, \quad (5)$$

where the wave functions of the two particles ($\beta\gamma$) in the (sd) shell are coupled and antisymmetrized to a state of total angular momentum J_1 and isospin T_1 , and the hole (α) is added to form the 2p-1h state of total angular momentum J and isospin T . These basis states are then mixed by the residual interaction.

The s.p. and s.h. energies were taken from the experimental level spectrum¹⁶ of ^{15}O and ^{17}O , and are listed in Table IV.

The particle-hole matrix elements were derived from Kuo-Brown particle-particle matrix elements

The level spectra of the $T=\frac{3}{2}$ odd-parity states up to $J=\frac{7}{2}$ and 16 MeV excitation which result from these calculations are shown in Fig. 9 together with the experimental spectrum for negative-parity states in ^{17}O . Case II gives better agreement than case I on an absolute energy scale. It also yields the correct spin sequence for the first five observed negative-parity states. However, it predicts (and so do all other calculations) a $\frac{1}{2}^-$ level near 14 MeV, which has not been found experimentally. This discrepancy will be discussed later.

The 2p-1h calculation of Margolis *et al.* gives predictions very similar to our case II. In their paper these authors renormalized the energies of their spectrum so as to put the first theoretical $J^{\pi}=\frac{1}{2}^-, T=\frac{1}{2}$ state at 3.10 MeV. However, it has been demonstrated since then¹² that the lowest $T=\frac{1}{2}$

where ϕ_i is the initial state with angular momentum and isospin J_i and T_i , respectively, ϕ_f is the final state with angular momentum and isospin J_f and T_f , respectively, and $E1$ represents the electric dipole operator $\frac{1}{2}\sum_i \tau_3 r Y_1$. Harmonic oscillator radial wave functions with $\hbar\omega = 41A^{-1/3}$ MeV were used. The final states, i.e., the ground state and first excited state were assumed to be good single-particle $1d_{5/2}$ and $2s_{1/2}$ states. Transfer reactions¹⁷ and neutron scattering data¹⁸ show that these states indeed contain most of the respective s.p. strength.

In Table VI the results of the present calculation for the transition strengths are compared with the experimental $B(E1)$ values. These were obtained from the expression $B(E1)(e^2\text{fm}^2) = \Gamma_\gamma(\text{eV})/1.05E_\gamma^3$ (MeV). For comparison, the simplest "single-particle" transition strengths are also included. These were computed by assuming a $(1p_{1/2}^{-1}2s_{1/2})$ excitation coupled with a $1d_{5/2}$ particle (for the γ_0 transition) or a $2s_{1/2}$ (for the γ_1 transition) particle to the appropriate initial state spins. While the experimental values represent the sums of γ_0 and γ_1 transitions the theoretical values for γ_0 and γ_1 are listed separately where possible (in the sequence γ_0, γ_1), and should be added for a comparison. On the other hand, the assumed simple structure of the single-particle transitions allows only γ_0 transition for the $\frac{3}{2}^-$ ($T = \frac{3}{2}$) single-particle state; therefore, all s.p. estimates are unique.

The first point to be made from Table VI is that the observed $B(E1)$ values are indeed hindered in the average tenfold with respect to the s.p. estimates. Secondly, both full-scale calculations reproduce this retardation and agree with experiment, except for the 14.174-MeV level. It should be remembered that the experimental error is generally about 50%, so that no real distinction can be made between cases I and II. Thirdly, the computed $B(E1)$ values for Soga's wave functions although reduced from the s.p. estimates do not reproduce the observed retardation. In Soga's wave function only one component can make an $E1$ transition so that the apparent reduction in the $B(E1)$ estimates from these wave functions is due to the renormalization of the wave functions for the different configurations included in them and not due to destructive interference from the different configurations that can form these states.

It has long been recognized and was first systematically investigated by Ejiri¹⁹ that first-forbidden decay matrix elements which involve the operator rY_1 are hindered by the same effects as the analogous $E1$ matrix element. In calculations which reproduce the experimental value for the $^{17}\text{N} \rightarrow ^{17}\text{O}$ β -decay rate, Towner and Hardy²⁰ and Zuker *et al.* (quoted in Ref. 20) obtain values which

correspond to $B(E1) = 14.0$ and 11.0 ($\times 10^{-3} e^2\text{fm}^2$), respectively, as compared with the present experimental value of 4.7 ± 2.0 ($\times 10^{-3} e^2\text{fm}^2$).

For the first $\frac{3}{2}^-$ level, we note that case I and case II give branching ratios of 36 and 48% to the first excited state, respectively, compared to the measured value of $(20 \pm 5)\%$.

As mentioned earlier, the single exception for agreement between theory and experiment is the transition from the state at $E_x = 14.174$ MeV which has been labeled $J^\pi = \frac{3}{2}^-$. Its transition strength is only slightly smaller than the s.p. value and is totally missed by our calculation. Soga fits the strength well. It was pointed out before that the effective interaction calculations predict a $J = \frac{1}{2}^-$ state very near the observed level, while the nearest predicted $\frac{3}{2}^-$ state lies about 1 MeV higher. If the spin is $\frac{1}{2}^-$, then the corrections in the integrated elastic proton scattering and radiative proton capture cross sections due to the spin effect lead to a $B(E1)$ value of $(42 \pm 28) \times 10^{-3} e^2\text{fm}^2$ which overlaps with the theoretical prediction of $13-17$ ($\times 10^{-3} e^2\text{fm}^2$) for the second $\frac{1}{2}^-$ state (see Table IV). The spin assignment from a comparison with the mirror nucleus ^{17}N is either $\frac{1}{2}^-$ or $\frac{3}{2}^-$. Either assignment is compatible with the elastic scattering results,³ although $J^\pi = \frac{3}{2}^-$ is favored at some angles.²¹ Although the radiative capture reaction in this region of excitation goes primarily by γ_0 emission it should be noted from Fig. 7 that the resonance is superimposed on a very large background. It is impossible from the present data to differentiate between a resonant γ_0 or γ_1 transition. Thus the over-all evidence for a $\frac{3}{2}^-$ assignment is quite weak, and the evidence from the transition strength appears to favor the $\frac{1}{2}^-$ spin assignment as this could make *all* transitions and the energy level spectrum consistent with theory.

V. CONCLUSIONS

The measured radiative $E1$ widths for the first five negative-parity $T = \frac{3}{2}$ states in ^{17}F demonstrate the systematic strong hindrance of these transitions with respect to single-particle estimates. This is in agreement with the general character of known $E1$ transitions from low-lying levels.

Microscopic 2p-1h calculations performed in a basis of good isospin reproduce the observed hindrance within the experimental errors for all transitions except one. The same calculation also gives a rather good account for the excitation energies, again with one exception. The single discrepancy would be removed by changing the spin assignment for the 14.174-MeV level from $\frac{3}{2}^-$ to $\frac{1}{2}^-$. This new assignment which is quite compatible with the elastic proton scattering data, would fit

this level into the general systematics.

As stated in the Introduction, the intent of this work is a consistent treatment of $E1$ transitions from both the low-lying and the collective states. The present calculations which fit the low-lying $E1$ strength distribution predicts collective states near 22 MeV, the region of the giant dipole resonance in ^{16}O . The experimental and detailed theoretical

results concerning the collective $E1$ strength distribution will be presented in the subsequent paper.

The authors would like to thank Professor A. Arima and Professor T. T. S. Kuo for many helpful discussions, and Professor P. D. Parker for communicating unpublished results.

*Work supported in part by the National Science Foundation.

† Present address: Physics Department, University of Washington, Seattle, Washington.

¹H. Ejiri, Nucl. Phys. A211, 232 (1973), and earlier references given therein.

²J. D. Vergados and T. T. S. Kuo, Nucl. Phys. A168, 225 (1971).

³B. M. Skwiersky, C. M. Baglin, and P. D. Parker, Phys. Rev. C 9, 910 (1974).

⁴R. G. Van Bree, Ph.D. thesis, Rutgers Univ., 1968 (unpublished).

⁵E. G. Adelberger, A. B. McDonald, C. L. Cocke, C. N. Davids, A. P. Shukla, H. B. Mak, and D. Ashery, Phys. Rev. C 7, 889 (1973).

⁶F. S. Dietrich, M. Suffert, A. V. Nero, and S. S. Hanna, Phys. Rev. 168, 1169 (1968).

⁷E. M. Diener, J. F. Amann, S. L. Blatt, and P. Paul, Nucl. Instrum. Methods 83, 115 (1970).

⁸E. G. Adelberger, A. B. McDonald, and C. A. Barnes, Nucl. Phys. A124, 49 (1969).

⁹W. A. Fowler, C. C. Lauritsen, and T. Lauritsen, Rev. Mod. Phys. 20, 236 (1948).

¹⁰R. F. Christy and W. A. Fowler, Phys. Rev. 96, 851 (1954).

¹¹I. Unna and I. Talmi, Phys. Rev. 112, 452 (1958).

¹²P. J. Ellis and T. Engeland, Nucl. Phys. A144, 161 (1970).

¹³B. Margolis and N. deTakacsy, Can. J. Phys. 44, 1431 (1966).

¹⁴M. Soga, Nucl. Phys. 89, 697 (1966).

¹⁵T. T. S. Kuo and G. E. Brown, Nucl. Phys. 85, 40 (1966); and private communication.

¹⁶H. P. Jolly, Jr., Phys. Lett. 5, 289 (1963).

¹⁷I. M. Naqib and L. L. Green, Nucl. Phys. A112, 76 (1968).

¹⁸C. H. Johnson and J. L. Fowler, Phys. Rev. 162, 890 (1967); Phys. Rev. C 2, 124 (1970).

¹⁹H. Ejiri, Nucl. Phys. A178, 350 (1971).

²⁰I. S. Towner and J. C. Hardy, Nucl. Phys. A179, 489 (1972).

²¹P. D. Parker, private communication.